Thermophoretically Augmented Mass Transfer Rates to Solid Walls Across Laminar Boundary Layers

Süleyman A. Gökoğlu* and Daniel E. Rosner†
Yale University, New Haven, Connecticut

Predictions of mass transfer (heavy vapor and small particle deposition) rates to solid walls, including the effects of thermal (Soret) diffusion ("thermophoresis" for small particles), are made by numerically solving the two-dimensional self-similar forced convection laminar boundary-layer equations with variable properties, covering the particle size range from vapor molecules up to the size threshold for inertial (dynamical nonequilibrium) effects. The effect of thermophoresis is predicted to be particularly important for submicron particle deposition on highly cooled solid surfaces, with corresponding enhancement factors at atmospheric conditions being over a thousand-fold at $T_w/T_e \approx 0.6$. As a consequence of this mass transfer mechanism, the particle size dependence of the mass transfer coefficient to a cooled wall will be much weaker than for the corresponding case of isothermal capture by Brownian-convective diffusion.

Nomenclature

C $= -\alpha_{T,-1}/\alpha_{T,\infty}$
c_p, c_v = specific heat at constant pressure and constant volume (per unit mass of mixture), respectively
d_p = particle diameter
D = Brownian diffusion coefficient
Eu = Euler number, $d\ln u_e/d\ln x$
f = dimensionless stream function
$-f_w$ = dimensionless wall blowing parameter
g-mer = cluster containing g monomer units ($g = 10^0, 10^1, \ldots, 10^{10}$)
j'' = diffusional mass flux of small particles
k = pseudo-first-order rate constant; Eq. (20)
Kn = Knudsen number (based on particle radius)
Le = Lewis number, Pr/Sc
M = molecular weight of the mixture
Ma = Mach number
p = pressure
Pr = Prandtl number (ratio of gas momentum diffusivity to heat diffusivity)
R = ideal gas constant
Re = Reynolds number
Sc = Schmidt number [ratio of gas momentum diffusivity to particle Brownian (Fick) diffusivity]
St = Stanton number; for either heat [Eq. (18)] or mass [Eq. (17)] transfer
T = absolute temperature
u, v = fluid velocity in x and y directions parallel and normal to wall, respectively
v_T = thermophoretic velocity; Eq. (19)
v_w = wall blowing velocity
W = normalized mass fraction of particles
x, y = distance along and normal to the surface
α_T = thermal diffusion factor of particle
$\alpha_{T,\infty}$ = thermal diffusion factor extrapolated to infinite temperature
$\alpha_{T,-1}$ = coefficient of T^{-1} in power series expansion of $\alpha_T(T)$
γ = heat capacity ratio, c_p/c_v, of gas mixture
δ = boundary-layer thickness
ϵ = Lennard-Jones molecular interaction energy (well-depth) parameter
η = dimensionless BL coordinate
θ = normalized temperature, T/T_e
κ = Boltzmann constant
λ = thermal conductivity of gas mixture
μ = dynamic viscosity of gas mixture
ξ = dimensionless, stretched boundary-layer coordinate (for Brownian diffusion sublayer); Eq. (14)
Ξ = function defined by Eq. (10a)
ρ = density of mixture
σ = Lennard-Jones molecular size parameter
Φ = function defined by Eq. (10b)
ψ = stream function; $\rho u = \partial\psi/\partial y$, $\rho v = -\partial\psi/\partial x$
ω = mass fraction of particles in prevailing mixture

Subscripts

e = outer edge of boundary layer (local mainstream)
eff = effective
ext = exterior region
h = heat transfer
int = interior region
g = g-mer
m = outer edge of mass transfer (Brownian diffusion) boundary layer or mass transfer
mom = momentum transfer
mp = melting point
p = particle
T = thermophoresis
w = at the surface, wall condition
x = quantity defined with respect to distance along x axis
1 = monomer molecule

Superscripts

α = temperature exponent in gas specific heat law
β = temperature exponent in gas viscosity law
ϵ = temperature exponent in gas thermal conductivity law
n = temperature exponent in Brownian diffusion coefficient law
$(\ )'$ = differentiation with respect to η

Miscellaneous

BL = boundary layer
BSL = Brownian sublayer
LBL = laminar boundary layer

Received Dec. 23, 1983; revision received May 29, 1985. Copyright © 1985 by D. E. Rosner. Published by the American Institute of Aeronautics and Astronautics with permission.

*Chemical Engineering Department; presently, Research Scientist, NASA Lewis Research Center, Cleveland, OH.

†Professor of Chemical Engineering and Applied Science; Director, High Temperature Chemical Reaction Engineering Laboratory.

I. Introduction

Due to the sharply increasing cost of high-grade fuels, there is renewed interest in the combustion of coal-derived or lower-grade petroleum-derived gas-turbine fuels containing inorganic impurities. Comprehensive but tractable design methods for predicting "ash" deposition rates, as well as precise and rapid methods of deposition rate measurement, are therefore needed.[1] Such results and techniques are also necessary to develop systems for "clean" hydrocarbon fuel combustion since 1) local fuel pyrolysis and inadequate oxidation rates can cause soot particle production and deposition; and/or 2) the "air" ingested for combustion may itself contain inorganic substances (e.g., sea salt and dust), which can deposit on gas-turbine components.[2]

Recognition of the engineering importance of *thermal diffusion mass transfer* ("thermophoresis" for small particles, which drift down a local temperature gradient) is relatively recent. The nearly linear increase in rate of small particle capture with the temperature difference (between the surface and mainstream gas) observed in recent experiments[3,4] is clearly due to thermophoresis[5,6] and not ordinary convective-(Brownian) diffusion or inertial impaction. For these reasons we have embarked on a series of theoretical studies of thermophoretically modified mass transfer in forced-, and natural-, convection systems. Forced-convection laminar boundary layers (LBLs) with variable fluid thermophysical properties and particle transport properties are treated in this paper, and mass transfer rate predictions are made based on rigorous numerical calculations for solid surfaces. We have considered a wide range of mainstream particle sizes, from vapor molecules up to small "aerosol" particles, with diameters of about 1 μm, above which inertial effects normally set in. (Inertial effects set in at a particle diameter that depends on the intrinsic particle density as well as the local aerodynamic—deceleration—environment; see, e.g., Ref. 6.) Our goal is to provide a set of reliable numerical results under reasonably simple, well-defined conditions. As will be seen, these results can be used to 1) define the conditions associated with large thermophoretic effects; and 2) develop and test simple correlations for including these phenomena in future engineering designs. In the present paper we focus on the formulation (Secs. II and III) and numerical solution (Sec. IV) of a number of prototypical LBL cases. Our results and a brief discussion of some of their implications conclude the paper (Secs. IV and V).

II. Mathematical Formulation

Boundary-Layer Equations

The boundary-layer (BL) conservation equations governing the velocity and temperature fields for the steady laminar flow of a viscous compressible fluid have been thoroughly reviewed.[7-10] Here, we consider also the mass transfer equation for a dilute ($\omega_e \ll 1$), nonreactive species, including thermophoresis. (The effects of the particles on the gas "host" flow[11] are neglected, as is the energy transport associated with particle fluxes,[12] because $\omega_e \ll 1$.) Given the two-dimensional (planar) configuration shown in Fig. 1, the full set of LBL equations takes the form

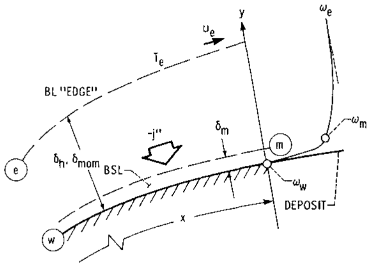

Fig. 1 Configuration and station nomenclature. Two-dimensional laminar boundary layer across which momentum, energy, and species mass are transferred by convection, diffusion, and (for species mass) thermophoresis; ($Sc \gg 1$).

Total mass:

$$\frac{\partial(\rho u)}{\partial x}+\frac{\partial(\rho v)}{\partial y}=0 \tag{1}$$

Streamwise momentum:

$$\rho\left(\frac{u\partial u}{\partial x}+\frac{v\partial u}{\partial y}\right)=\frac{\partial(\mu\partial u/\partial y)}{\partial y}-\frac{\mathrm{d}p}{\mathrm{d}x} \tag{2}$$

Energy:

$$\rho c_p\left(\frac{u\partial T}{\partial x}+\frac{v\partial T}{\partial y}\right)=\frac{\partial(\lambda\partial T/\partial y)}{\partial y}+\mu\left(\frac{\partial u}{\partial y}\right)^2+\mathrm{u}\left(\frac{\mathrm{d}p}{\mathrm{d}x}\right) \tag{3}$$

Species mass:

$$\rho\left(\frac{u\partial\omega}{\partial x}+\frac{v\partial\omega}{\partial y}\right)=\frac{\partial}{\partial y}\left\{\rho D\left[\frac{\partial\omega}{\partial y}+\frac{\alpha_T\omega}{T}\frac{\partial T}{\partial y}\right]\right\} \tag{4}$$

In the above equations (1-4) the constitutive equation of state is taken to be the ideal gas law ($p=\rho RT$), and the local pressure field is assumed to vary only in the streamwise direction ($\mathrm{d}p/\mathrm{d}x=-\rho_e u_e/\mathrm{d}x$). Of particular interest in this work is the influence of thermophoresis [second term, right-hand side of Eq. (4)] on the rate of mass transport to the cooled, solid surface.

Boundary Conditions

Consider a smooth solid wall with constant (x-independent) temperature. The wall is assumed to be cool (or "sticky") enough to act as a perfect particle sink. The terms deposition rate and particle arrival rate are therefore used interchangeably. If we neglect the local gas phase concentration of particles ω_w (cf. ω_e), the wall boundary conditions become

At $y=0$:

$u=0$, $v=0$ (or v_w for wall transpiration cooling)‡

$$T=T_w, \quad \omega=0 \tag{5a}$$

Moreover, in the "dusty" gas "far" from the surface, we impose

$$\text{At } x=0 \text{ and/or } y\to\infty: \quad u\to u_e, \quad T\to T_e, \quad \omega\to\omega_e \tag{5b}$$

As evident from Eq. (4), our species mass conservation equation does not contain an explicit local source or sink term since we are considering the limit of a "frozen" BL, i.e., no chemical reaction, nucleation, condensation, coagulation, or particle breakup is presumed to occur within the BL. Therefore, the results we report can be applied even if the mainstream has a distribution of particle size classes (g-mers), each containing the number g ($g=10^0, 10^1, \ldots, 10^{10}$) monomer units,§ provided the particle concentrations

---

‡The simultaneous effects of thermophoretic "suction" and real blowing (through the wall) are treated elsewhere.[13,14]

§For the numerical results reported here, we have used the following estimated properties of Na_2SO_4 (monomer molecular weight $=142.04$, $\sigma=5.00$ Å, $\epsilon/\kappa=2221$ K, $\alpha_{T,\infty}=0.7765$, $C=458.6$ K; $T_{mp}=1157$ K, $\rho_{mp}=2$ g/cm^3, $\lambda_p=10^{-3}$ cal/cm-sec-K); however, thermophoretic BL calculations done for SiO_2 and C g-mers, using estimated properties of their monomers, indicate that the detailed physical and chemical properties of g-mers have no appreciable effect on the resulting small particle convective-diffusion deposition rates.[15] Thus, the numerical results reported here are not expected to be applicable only to $Na_2SO_4(c)$-like particles.

are such that transport to the wall occurs without appreciable mutual interaction.

Property Variations and Similarity Transformations

For carrier fluid and transported species property variation estimates, the temperature dependencies are chosen as follows:

$$\mu \sim T^{\beta},\ \lambda \sim T^{\epsilon},\ c_p \sim T^{\alpha},\ \rho \sim T^{-1},\ D \sim T^{n},$$

$$\alpha_T \cong \alpha_{T,\infty} \cdot [1-(C/T)]$$

Details for the selection of the best powers of temperature, β, ϵ, α, and n are given in Refs. 15 and 16 ($\beta = 0.70$, $\epsilon = 0.85$, $\alpha = 0.19$ and, for Na_2SO_4 monomer, $n = 1.66$ are reasonable estimates when air is the host gas). The calculations of D and α_T for monomers and g-mers (considered here simply as heavy molecules) are given in the Appendix. The additional parameters Sc, Pr, Ma_e, γ_e, and Eu are defined by

$$Sc \equiv \frac{\mu/\rho}{D}, \quad Pr \equiv \frac{\mu/\rho}{\lambda/(\rho c_p)}$$

$$Ma_e^2 \equiv \frac{u_e^2}{\gamma_e R T_e/M}, \quad \gamma_e \equiv \left(\frac{c_p}{c_v}\right)_e, \quad Eu \equiv \frac{d\ell n u_e}{d\ell n x}$$

We also introduce the following nondimensional dependent variables:

$$W \equiv \omega/\omega_e, \quad \theta \equiv T/T_e, \quad f \equiv \psi/(\mu_w \rho_w x u_e)^{1/2}$$

These will be assumed below to be functions of the single nondimensional ("similarity") coordinate η, where

$$\eta \equiv y(\rho_w u_e/\mu_w x)^{1/2} = (y/x)\cdot(Re_x)_w^{1/2}$$

With $\theta_w \equiv T_w/T_e$ and noting that $u/u_e = (\rho_w/\rho)\cdot f'$, we find

Streamwise momentum:

$$\begin{aligned} f''' = {} & (Eu)\cdot(\theta_w^{\beta}\theta^{-\beta} f'^2 - \left[\frac{1+Eu}{2}\right]\theta_w^{\beta}\theta^{-\beta} f'' f \\ & - (Eu)\cdot\theta_w^{\beta+2}\theta^{-\beta-1} - \left[\frac{1+Eu}{2}\right]\theta_w^{\beta}\theta^{-\beta-1}\theta' f' f \\ & - \left(\frac{\theta''}{\theta}\right) f' - (\beta+2)\left(\frac{\theta'}{\theta}\right) f'' - \beta\left(\frac{\theta'}{\theta}\right)^2 f' \end{aligned} \tag{6}$$

Energy:

$$\begin{aligned} \theta'' = {} & -\left[\frac{1+Eu}{2}\right] Pr_w \theta_w^{\epsilon-\alpha} f \theta^{\alpha-\epsilon}\theta' - \frac{\epsilon\theta'^2}{\theta} \\ & + Ma_e^2(\gamma_e - 1) Pr_w \theta_w^{\epsilon-\alpha}\theta^{1-\epsilon}[(Eu)f' - \theta_w^{-2-\beta} f''^2 \theta^{\beta+1} \\ & - 2\theta_w^{-2-\beta} f'' f' \theta^{\beta}\theta' - \theta_w^{-2-\beta} f'^2 \theta^{\beta-1}\theta'^2] \end{aligned} \tag{7}$$

Species mass:

$$\begin{aligned} & W'' + \left\{ Sc_w \left[\frac{1+Eu}{2}\right]\theta_w^{n-1}\theta^{1-n} f + \frac{(n-1+\alpha_T)\theta'}{\theta} \right\} W' \\ & + \{(\alpha_T/\theta)[\theta'' + (n-2+C/(T-C))\theta'^2/\theta]\} W = 0 \end{aligned} \tag{8}$$

and the transformed boundary conditions are

At $\eta = 0$: $f = 0$ (or f_w for wall transpiration cooling)

$$f' = 0, \quad \theta = T_w/T_e, \quad W = 0 \tag{9a}$$

As $\eta \to \infty$: $f' \to T_w/T_e$, $\theta \to 1$, $W \to 1$ (9b)

Although one of the boundary conditions specifies behavior as $\eta \to \infty$, in practice this condition can be satisfied at a large but finite value of η, corresponding to a dimensionless BL thickness.

III. Asymptotic Analysis for $\alpha_T[(T_e/T_w) - l] \gg 1$

The analysis given above covers the particle size range from vapor molecules [$Sc = \mathcal{O}(1)$] to about 1-μm-diam particles [$Sc = \mathcal{O}(10^6)$]. It is known that in the absence of thermophoresis the ratio of the thickness of the momentum BL, δ_{mom}, to the thickness of the mass transfer BL, δ_m, scales with $(Sc)^{1/3}$. Therefore, as the particle size, and hence Sc increases, the mass transfer BL becomes completely embedded within the momentum (energy) transfer BL. In the presence of thermophoresis, however, mass transfer starts as soon as the particles experience temperature gradients. The concentration gradient created by the thermophoretic motion of the particles, in turn, induces Brownian diffusion. Strictly speaking, therefore, for coupled thermophoretic and diffusive mass transport of small particles ($Sc > 1$) the mass transfer BL thickness is the same as the energy transfer BL thickness, δ_h. Yet, for thermophoretically dominated mass transport, a simplified asymptotic analysis is possible.[17,18] The mass transfer BL can then be visualized as one exterior region where the mass transport mechanisms are basically convection and thermophoresis (negligible Brownian diffusion) and one interior region with thickness δ_m, which we call the Brownian diffusion sublayer, where Brownian diffusion also becomes important (Fig. 1). The mathematical treatment follows.

Exterior Region

The species mass conservation equation can be rewritten in the form

$$(1/Sc_w)W'' + \Xi W' + \Phi W = 0 \tag{10}$$

where

$$\Xi \equiv [(1+Eu)/2][\theta^{1-n}\theta_w^{n-1} f] + [(n-1+\alpha_T)/Sc_w](\theta'/\theta) \tag{10a}$$

and

$$\Phi \equiv [\alpha_T/(Sc_w\theta)]\{\theta'' + [n-2+C/(T-C)](\theta'^2/\theta)\} \tag{10b}$$

It is known that the thermophoretic-to-momentum diffusivity ratio α_T/Sc remains $\mathcal{O}(1)$ regardless of how large Sc is.[18-20] Therefore, even slight temperature gradients are sufficient[14] for thermophoresis to dominate over Brownian diffusion for small particles ($Sc \gg 1$ and $\alpha_T[(T_e/T_w) - 1] \gg 1$). This can be readily seen by comparing the second-order Brownian diffusion term in Eq. (10) with the thermophoretic term [the second term in Eq. (10a)]. The species mass conservation equation in this region can be reduced to a first-order ordinary differential equation by neglecting the concentration diffusion term. In so doing, however, we must give up satisfying the wall boundary condition $W_w = 0$. The solution to the reduced equation can therefore be expressed in the quadrature form

$$W_{ext}(\eta) = \exp\left[\int_{\eta}^{\infty} \frac{\Phi(\eta)}{\Xi(\eta)} d\eta\right] \tag{11}$$

When formally evaluated at $\eta = 0$, the above integral defines the useful quantity W_m, which is the normalized mass fraction of the transported particles at the outer edge of the Brownian diffusion sublayer, where the exterior and the interior solutions are to be matched;[21] i.e.,

$$W_m \equiv W_{\text{ext}}(0) = \exp\left[\int_0^\infty \frac{\Phi(\eta)}{\Xi(\eta)} d\eta\right] \tag{12}$$

Interior Region (Brownian Diffusion Sublayer)

Since the interior region is very thin, it is permissible to assume constant coefficients (evaluated at the wall) therein. The species mass conservation equation, then, takes the simple form

$$(1/Sc_w)W'' + \Xi(0)W' + \Phi(0)W = 0 \tag{13}$$

In order that the wall boundary condition ($W_w = 0$) be satisfied, the concentration gradients will be very large in this thin region. Therefore, it is mathematically convenient to stretch the coordinate η by the factor $Sc_w\Xi(0)$ and define the new independent variable ξ:

$$\xi \equiv Sc_w\Xi(0)\eta$$

In terms of ξ, Eq. (13) becomes

$$\frac{d^2W}{d\xi^2} + \frac{dW}{d\xi} + \left[\frac{\Phi(0)}{Sc_w\Xi(0)^2}\right]W = 0 \tag{14}$$

Since $\alpha_T[(T_e/T_w) - 1)] \gg 1$, we can clearly neglect the pseudosource (sink) term. The resulting reduced equation, along with its boundary conditions

at $\xi = 0$, $W = 0$

at $\xi \to \infty$, $W \to W_m$ (matching condition with exterior solution) (15)

can be solved to give

$$W_{\text{int}}(\xi) = W_m[1 - \exp(-\xi)] \tag{16a}$$

The corresponding gradient at the wall is found to be

$$W'_w = W'(0) = Sc_w \cdot \Xi(0) \cdot W_m \tag{16b}$$

It is worthwhile at this point to comment on some of the direct consequences of the asymptotic analysis:

Comment 1

The mass (deposition) flux at the wall is given by ($\omega_w = 0$):

$$-j''_w = \rho_w D_w\left[\left(\frac{\partial\omega}{\partial y}\right)_w + \frac{\alpha_{T,w}\omega_w}{T_w}\left(\frac{\partial T}{\partial y}\right)_w\right]$$
$$= \rho_w D_w\left(\frac{\partial\omega}{\partial y}\right)_w = \rho_e u_e St_m \omega_e \tag{17}$$

It can be seen from Eq. (17) that although the thermophoretic flux term (second term in the brackets) has no direct contribution to the deposition flux (because $\omega_w = 0$), it indirectly affects the deposition flux by changing the concentration profile and thereby modifying $(\partial\omega/\partial y)_w$. In fact, although Brownian diffusion is completely neglected in the exterior region, it eventually takes over in the interior region, becoming the *only* mass transfer mechanism *at* the surface.

Comment 2

For thermophoretically dominated mass transport, the deposition flux is approximated in the literature[17,18,22,23] by

$$-j''_w \cong -j''_m = \rho_m D_m\left(\frac{\partial\omega}{\partial y}\right)_m - \rho_m v_{T,m}\omega_m \cong -\rho_m v_{T,m}\omega_m$$
$$= \rho_m D_m \alpha_{T,m}\left(\frac{\partial \ell n T}{\partial y}\right)_m \omega_m \cong \rho_e u_e(\alpha_T Le)_w St_h\left[\frac{T_e - T_w}{T_w}\right]\omega_m \tag{18}$$

where v_T is the thermophoretic velocity defined by

$$v_T \equiv -D\alpha_T\left(\frac{\partial \ell n T}{\partial y}\right) \tag{19}$$

Comparison of Eqs. (17) and (18) reveals that because the Brownian diffusion sublayer thickness δ_m is very small, the mass fluxes calculated at station ⓜ or at station ⓦ (Fig. 1) both give approximately the same result. The asymptotic analysis is a mathematical justification of this approximation. In fact, Eq. (16a) simply states that the concentration gradient at the wall is adjusted in the interior region (BSL) such that the Brownian diffusion flux alone at station ⓦ can accommodate the incoming thermophoretic flux from the exterior region at station ⓜ. Therefore, as a corollary, one can say that the mass flux to the wall [Eq. (16b) or Eq. (18)] can be easily evaluated from an integral [Eq. (12)] that is only a function of behavior outside the Brownian diffusion sublayer.

Comment 3

Another interesting outcome of the asymptotic analysis is that the Brownian diffusion sublayer is confined to a much thinner region whenever thermophoresis is significant ($\alpha_T[(T_e/T_w) - 1] \gg 1$). Indeed, the ratio of its thickness to the momentum transfer BL thickness now scales like Sc^{-1} [Eq. (16b)] as compared to $Sc^{-1/3}$ in the absence of thermophoresis and, consequently, the concentration gradient in this region is now much steeper.

IV. Results and Discussion

The LBL equations in the transformed coordinate system have been first subjected to a Newton quasilinearization.[24] Then the linearized, coupled momentum and energy equations have been finite differenced and solved simultaneously by inverting the resulting tridiagonal matrices to obtain self-consistent velocity and temperature profiles. Having these, the coefficients Ξ and Φ of the species equation are evaluated at each mesh point and the linear species equation is separately solved by inverting the tridiagonal matrix resulting from its finite difference form. To evaluate the concentration gradient at the wall, the program utilizes the asymptotic analysis for $Sc \gtrsim 10^3$¶ to preserve accuracy.** Although the formulation is kept general, it is illustrated here only for cases with $Ma_e^2 \ll 1$. The interesting effects of viscous dissipation on thermophoresis are treated elsewhere.[25]

The numerical accuracy of our LBL program has been checked in the following limits, with excellent agreement with the cited references:

1) Velocity and temperature profiles with constant and variable properties.[26-32]

2) Concentration profiles with or without thermophoresis, with and without variable fluid properties.[17,33]

¶The highest Sc at which the program switches to the asymptotic solution depends upon the mesh size used. That is, at the switch-point the Brownian diffusion sublayer is so "thin" that, for the given mesh size, the numerical results are no longer accurate; but Sc and $\alpha_T[(T_e/T_w) - 1]$ are large enough to assure the accuracy of the asymptotic solution in predicting W_m and the corresponding concentration gradient at the wall.

**For a more detailed description of the program, including its convergence characteristics, accuracy, mesh size used, quasilinearization, and finite differencing, see Ref. 15.

Table 1 lists the eigenvalues for a number of representative numerical integrations.

If the differentiation on the right-hand side of Eq. (4) is formally carried out, the presence of thermophoresis is found to introduce a suction-like convective term proportional to the thermophoretic velocity v_T Eq. (19), and a source-like term proportional to an effective first-order reaction rate constant[5]

$$k_{\text{eff}} \equiv \left(\frac{1}{\rho}\right)\cdot\frac{\partial}{\partial y}\,\frac{\rho D\alpha_T \partial \ln T}{\partial y} \qquad (20)$$

Therefore, Eq. (4) can now be rewritten in the "transparent" form

$$\frac{\rho u\partial\omega}{\partial x}+\frac{\rho(v+v_T)\partial\omega}{\partial y}=\frac{\partial}{\partial y}\left(\frac{\rho D\partial\omega}{\partial y}\right)+\rho k_{\text{eff}}\,\omega \qquad (21)$$

which proves useful in anticipating, correlating, and discussing the effects of thermophoresis on composition profiles and local mass transfer rates.[5]

For heavier particles (cf. the carrier gas) depositing on cold walls (the case of interest here), the suction effect of thermophoresis is found to dominate the sink effect, dramatically augmenting overall total deposition rates. Even though the Brownian diffusion sublayer is completely buried inside the heat and momentum transfer BLs ($\delta_m \ll \delta_h \approx \delta_{\text{mom}}$), as soon as large particles ($Sc \gg 1$) enter the thermal BL, the suction [Eq. (19)] and the sink [Eq. (20)] effects of thermophoresis start to operate in response to the local temperature gradients. This results in a nonzero thermophoretic velocity normal to the surface, and a reduced particle concentration ω_m (instead of the mainstream value ω_e) at the outer edge of the Brownian diffusion sublayer (Fig. 1).

Figures 2-4 summarize our numerical results obtained from the solution of the LBL equations (including particle thermophoresis) for a solid wall with negligible viscous dissipation over a wide range of particle diameters to about 1 μm. For still larger particles, where inertial effects often set in, predictions can be made using the recent results of

Table 1 Summary of numerical results for selected LBL integrations[a]

T_w/T_e	g	Sc_w	$\alpha_{T,w}$	Eu	p(atm)	W'_w	$W'_{w,0}$[b]	θ'_w	f''_w
0.6	10^0	1.919	0.381	1	20	0.713	0.679	0.189	0.966
↓	10^1	5.112	2.838	↓	↓	1.228	0.944	↓	↓
	10^2	21.87	12.26			3.316	1.598		
	10^3	97.27	53.81			12.43	2.575		
	10^4	435.7	235.3			53.12	4.245		
	10^5	1854.4	968.2			220.0	6.880		
	10^6	6532.9	3239.5			746.1	10.47		
	10^7	17394.0	7733.9			1872.2	14.51		
	10^8	39601.3	14554.9			3755.1	19.09		
	10^9	86305.8	25509.8			6897.0	24.75		
	10^{10}	186361.3	46093.7			12786.5	31.99		
0.8	10^0	1.839	0.480	1	20	0.713	0.696	0.0955	1.103
↓	↓	↓	↓	0	20	0.415	0.404	0.0583	0.324
				1	1	0.713	0.696	0.0955	1.103
	10^1	5.535	3.080	1	20	1.170	1.032	↓	↓
	↓	↓	↓	0	20	0.667	0.581		
			3.096	1	1	1.170	1.032		
	10^2	23.81	13.39	1	20	2.518	1.740		
	↓	↓	↓	0	20	1.437	0.954		
		23.82	13.54	1	1	2.527	1.740		
	10^3	106.2	59.18	1	20	7.239	2.841		
	↓	↓	↓	0	20	4.259	1.563		
		106.5	60.59	1	1	7.350	2.844		
	10^4	480.1	262.2	1	20	28.19	4.698		
	↓	↓	↓	0	20	17.00	2.584		
		485.4	275.9	1	1	29.47	4.715		
	10^5	2117.3	1123.2	1	20	118.7	7.705		
	↓	↓	↓	0	20	71.99	4.237		
		2234.0	1265.9	1	1	132.9	7.844		
	10^6	8231.1	4200.9	1	20	445.7	12.11		
	↓	↓	↓	0	20	270.3	6.663		
		10325.1	5814.1	1	1	610.7	13.07		
	10^7	24413.0	11605.2	1	20	1245.4	17.41		
	↓	↓	↓	0	20	755.8	9.573		
		47743.0	26561.4	1	1	2793.8	21.77		
	10^8	58067.5	23960.8	1	20	2620.1	23.23		
	↓	↓	↓	0	20	1591.9	12.78		
		219185.0	119425.6	1	1	12589.9	36.18		
	10^9	127869.6	43747.5	1	20	4865.3	30.23		
	↓	↓	↓	0	20	2958.7	16.63		
		968249.2	511972.0	1	1	54120.2	59.36		
	10^{10}	276689.9	80041.4	1	20	8997.5	39.10		
	↓	↓	↓	0	20	5473.9	21.50		
		3700280.6	1879546.1	1	1	199554.1	92.80		

[a] Eigenvalues pertain to Na_2SO_4 g-mers in air with a mainstream temperature of $T_e = 1500$ K.
[b] $W'_{w,0}$ values pertain to $\alpha_T = 0$ (no thermophoresis).

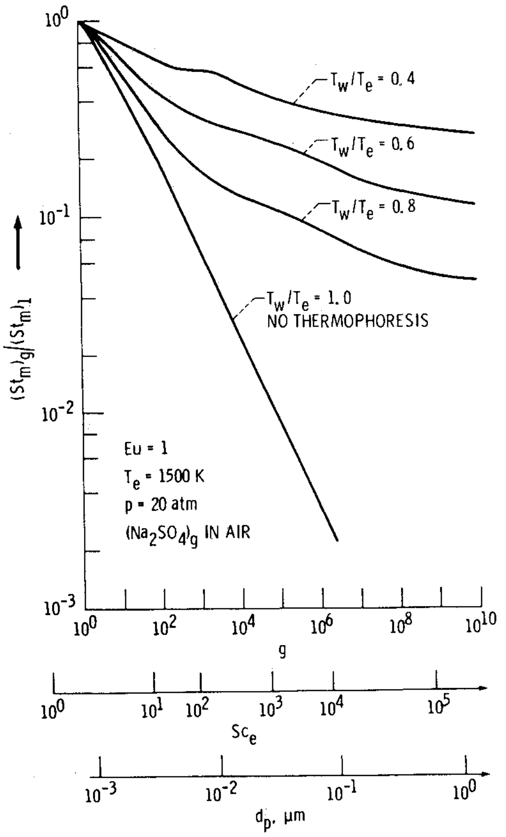

Fig. 2 Predicted dependence of mass transfer coefficient on particle size and temperature ratio; laminar boundary-layer stagnation point (two-dimensional); $p = 20$ atm, $T_e = 1500$ K.

Rosner, Fernandez de la Mora, and Israel.[34-38] In Fig. 2 the dimensionless mass transfer Stanton number (St_m), for a given size particle, is normalized with the corresponding vapor St_m value on the ordinate. It is known that thermal (Soret) mass diffusion has a relatively small effect (a few percent) on such deposition rates;[2,5] therefore, the figure depicts how much mass transfer can be altered (increased) due to thermophoresis for a certain size particle by simply reducing the temperature ratio, T_w/T_e (colder wall). The $T_w/T_e = 1$ curve corresponds to deposition rate predictions in the absence of thermophoresis and, as can be seen from the figure, 1) the error involved in neglecting thermophoresis becomes very serious indeed, as the particles become larger, and 2) thermophoresis reduces the usual sensitivity of the mass transfer coefficient to particle size.

In Fig. 3 we display three different phenomena:

1) The ordinate is proportional to the deposition rate but is normalized in such a way that if one neglects thermophoresis, then the quantity $W_w' Sc_w^{-1/3}$ is a constant for all particle sizes, pressures, and temperature ratios (to the extent variable properties influence it) for each Euler number (Eu). Hence, the departure of the curves from their corresponding horizontal (constant) lines is due to thermophoresis.

2) Pressure affects total deposition rates through the dependency of particle transport properties on pressure. At ordinary pressures the particle sizes of interest here cover the range from the free molecular regime ($Kn_p \gg 1$), where Chapman-Enskog theory is applicable, to the continuum regime ($Kn_p \ll 1$), where Stokes-Einstein theory holds. By virtue of the transition between those two regimes the particles experience a denser or more rarefied environment, depending on pressure and temperature level. Particles in high-pressure environments (e.g., in modern gas turbines) enter the transition regime earlier (i.e., at smaller sizes) and reach the continuum regime earlier than particles of the same size, subject to lower (say, atmospheric) pressures. Particle Schmidt number Sc and thermophoretic diffusivity $\alpha_{T,p} D_p$ decrease with increasing pressure in the transition-to-continuum

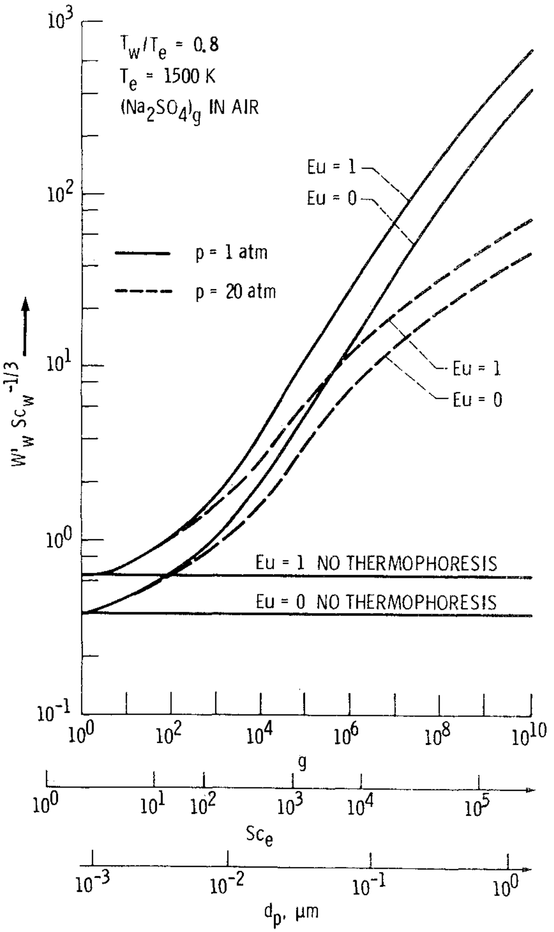

Fig. 3 Predicted dependence of Na_2SO_4 deposition rate on particle size, Euler number, and pressure in a laminar boundary layer at $T_w/T_e = 0.8$.

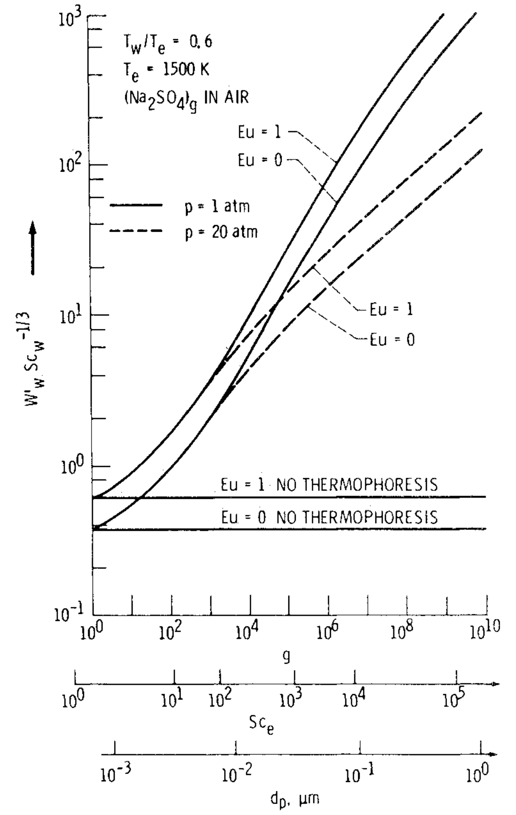

Fig. 4 Predicted dependence of Na_2SO_4 deposition rate on particle size, Euler number, and pressure in a laminar boundary layer at $T_w/T_e = 0.6$.

regime, resulting in a reduction of the enhancement of mass transfer due to thermophoresis at any particular T_w/T_e value.

3) Calculations done for the forward stagnation point ($Eu=1$) and flat plate ($Eu=0$) show that the Euler number has no appreciable effect on the thermophoretic enhancement of mass transfer.

In closing, we note that even at $T_w/T_e=0.8$, thermophoresis increases the deposition rate of about 1 μm diameter particles ($Sc \simeq 10^6$) by about a thousandfold at $p=1$ atm on a solid object. The enhancement is even more dramatic for colder walls (e.g., $T_w/T_e=0.6$) in Fig. 4, having the same characteristics as Fig. 3.

V. Concluding Remarks

Numerical calculations, reported here for self-similar two-dimensional LBLs with variable properties, covering the particle size range from vapor molecules to the threshold size for the onset of inertial effects, demonstrate the engineering importance of the thermophoretic mass transport mechanism, especially for submicron particle deposition on cooled walls. In fact, for particle Schmidt numbers above about 10^3, the mass transport rate to a cold wall is dominated by thermophoresis (the enhancement being approximately a thousandfold for approximately 1 μm diam particles at $T_w/T_e=0.8$ and $p=1$ atm). The mass transfer ratio associated with thermophoresis was found to be insensitive to the Euler number Eu, i.e., local pressure gradient, although the pressure level itself is significant since it determines the effective particle thermophoretic diffusivity in the transition and continuum regimes ($Kn_p<1$). Many features of our predictions and those of Ref. 17 remain to be experimentally verified; however, the magnitude of the (three-decade) augmentation ratio and the dependence of particle deposition rate on wall-to-gas temperature ratio have recently been verified in the seeded laboratory flat flame experiments of Rosner and Kim,[4] albeit at lower Reynolds numbers than those assumed in the present paper ($Re^{1/2} \gg 1$).

To incorporate these mass transfer effects in engineering design calculations, it is of course useful to economically summarize the results of such numerical LBL integrations in simple but rational correlation equations. For this reason, results of the numerical calculations presented here, as well as the similar ones that also include the effects of viscous dissipation,[25] transpiration cooling and hot walls[39] for BLs that are self-similar,[13] law-of-the-wall turbulent,[14] and developing (allowing for laminar-to-turbulent transition[40]), also serve as a base against which the accuracy and the applicability limits of simple engineering correlations[41,42] are being tested. A detailed discussion of the structure and use of these correlations is beyond the scope of the present paper; however, it can be stated that 1) they follow immediately from the pseudosuction/pseudosink viewpoint[5] described briefly in Sec. IV and 2) results obtained to date[41,42] are encouraging, even when applied locally to developing (e.g., gas-turbine blade) boundary layers.[40]

Appendix: Calculation of Species Transport Properties

We assume that the transport coefficients for each vapor species (monomers) depend on local pressure and temperature via first-order Chapman-Enskog theory with estimated Lennard-Jones 12:6 interaction parameters.[43,44] For trace species the (dimensionless) thermal diffusion factor and the Fick (Brownian) diffusion coefficient are thus independent of mole fraction. The thermal diffusion factor is given by rather lengthy expressions in the literature.[45] We therefore fit each calculated monomer α_T value by a two-parameter expression $\alpha_T=\alpha_{T,\infty}(1-C/T)$. These parameters, $\alpha_{T,\infty}$ and C, for many vapor/carrier combinations of engineering interest are given in Refs. 5 and 46, where it is shown that the molecular weight disparity between the transported trace substance and the host fluid dictates the magnitude of $\alpha_{T,\infty}$.

For the calculation of the thermal diffusion factor of small particles, the expression developed by Talbot et al.[20] is used in the form

$$\alpha_{T,p}=\{[(3/4)Sc][3.12(\mathrm{SCF})][\lambda/\lambda_p + 2.18Kn]\}/\{(1+3\cdot 42Kn)[1+4.36Kn+2(\lambda/\lambda_p)]\} \tag{A1}$$

where SCF is the Stokes-Cunningham factor given by

$$\mathrm{SCF}=1+Kn[1.246+0.42\exp(-0.88/Kn)] \tag{A2}$$

and λ is the host gas translational thermal conductivity.

The thermal diffusion factor of a cluster consisting of g molecules (g-mer) is then evaluated by interpolating the values obtained for a monomer and from Eq. (A1). The interpolation formula we adopted is

$$\alpha_{T,g}=\{1/[1+b(g-1)]\}\alpha_{T,\mathrm{monomer}} + \{b(g-1)/[1+b(g-1)]\}\alpha_{T,p} \tag{A3}$$

By taking the value of b to be 5, we forced the thermal diffusion factor of the cluster to reach 98% of the particle value $\alpha_{T,p}$ when the number of molecules in the cluster, g, reached 10.

It is assumed that $\alpha_{T,g}$ has the same temperature dependency as the monomer. Two sets of $\alpha_{T,\infty,g}$ and C parameters are calculated between T_w and $(T_w+T_e)/2$, and $(T_w+T_e)/2$ and T_e to describe the temperature dependency more accurately.

For the calculation of the Brownian diffusion coefficient of the g-mer we first obtain two different diffusion coefficients for the g-mer: one is evaluated using the Chapman-Enskog theory ($D_{g,CE}$) for low density ($Kn \gg 1$) gases, and the other is evaluated using the Stokes-Einstein theory ($D_{g,SE}$) for $Kn \ll 1$. We then adopt an interpolation formula given as

$$[(D_1/D_g)-1]=\{[(D_1/D_{g,CE})-1][(D_1/D_{g,SE})-1]\} \div \{[(D_1/D_{g,CE})-1]^{2.14}+[(D_1/D_{g,SE})-1]^{2.14}\}^{1/2.14} \tag{A4}$$

where D_1 is the Fick (Brownian) diffusion coefficient of the monomer calculated from Chapman-Enskog theory.[43] The exponent 2.14 was selected to force agreement between D_g given by Eq. (A4) and the slip-corrected value of $D_{g,SE}$ at the particle Knudsen number of unity. The calculation of n to describe the temperature dependency of $D_g \sim T^n$ is given in detail in Ref. 16.

Acknowledgments

We are indebted to the U.S. Air Force Office of Scientific Research—Air Breathing Combustion/Propulsion Division and to NASA-Lewis Research Center for their support of this research, under Contract F49620-82K-0020 and Grant NAG 3-201 at Yale University, respectively. We have also benefited from useful discussions and/or correspondence with Drs. J. Fernandez de la Mora, R. Israel (Yale University), R. Wenglarz (Allison Division—General Motors Corp.) and F. J. Kohl (NASA-Lewis Research Lab).

References

[1] Rosner, D. E. and Seshadri, K., "Experimental and Theoretical Studies of the Laws Governing Condensate Deposition from Combustion Gases," *Eighteenth (International) Symposium on Combustion*, The Combustion Institute, 1981, pp. 1385-1394.

[2] Rosner, D. E., Chen, B. K., Fryburg, G. C., and Kohl, F. J., "Chemically Frozen Multicomponent Boundary Layer Theory of Salt and/or Ash Deposition Rates from Combustion Gases," *Combustion Science and Technology*, Vol. 20, 1979, pp. 87-106.

[3] Nomura, M., Morishita, T., and Kan, S., "An Experiment of Deposit Formation on Surface of an Air Cooled Gas Turbine

Blade," *Proceedings of the 1977 Tokyo Joint Gas Turbine Congress*, 1977, JSME/ASME, pp. 566-573.

[4] Rosner, D. E. and Kim, S. S., "Optical Experiments on Thermophoretically Augmented Submicron Particle Deposition from "Dusty" High Temperature Gas Flows," *Chemical Engineering Journal*, Vol. 29, 1985, pp. 147-157.

[5] Rosner, D. E., "Thermal (Soret) Diffusion Effect on Interfacial Mass Transport Rates," *PhysicoChemical Hydrodynamics Journal*, Vol. 1, 1980, pp. 159-185.

[6] Vermes, G., "Thermophoresis-Enhanced Deposition Rates in Combustion Turbine Blade Passages," *Transactions of the ASME Journal of Engineering for Power*, Vol. 101, 1979, pp. 542-548.

[7] Schlichting, H., *Boundary Layer Theory*, 6th ed., McGraw-Hill Book Co., New York, 1968.

[8] Stewartson, K., *The Theory of Laminar Boundary Layers in Compressible Fluids*, Oxford University Press, London/NY, 1964.

[9] Evans, H. L., "Laminar Boundary Layer Theory, Addison-Wesley, London, 1968.

[10] Batchelor, G. K., *An Introduction to Fluid Dynamics*, Cambridge University Press, London, 1967.

[11] Rosner, D. E., Castillo, J., and Park, H. M., "Thermophoretically-Modified Momentum, Energy and Mass Transfer Coefficients for the Laminar Boundary Layer Flow of High Mass Loaded Particle-Containing Gases," in preparation, 1985.

[12] Atimtay, A. and Gill, W. N., "The Effect of Free Stream Concentration on Heat and Binary Mass Transfer with Thermodynamic Coupling in Forced Convection on a Flat Plate," *Chemical Engineering Science*, Vol. 36, 1981, pp. 1001-1008.

[13] Gökoğlu, S. A. and Rosner, D. E., "Effect of Particulate Thermophoresis in Reducing the Fouling Rate Advantages of Effusion-Cooling," *International Journal of Heat and Fluid Flow*, Vol. 5, No. 1, 1984, pp. 37-41.

[14] Gökoğlu, S. A. and Rosner, D. E., "Thermophoretically Enhanced Mass Transport Rates to Solid and Transpiration-Cooled Wall Across Turbulent (Law-of-the-Wall) Boundary Layers," *Industrial Engineering Chemistry-Fundamentals*, Vol. 24, No. 2, 1985, pp. 208-214.

[15] Gökoğlu, S. A., *Thermophoretically Enhanced Deposition of Particulate Matter Across Nonisothermal Boundary Layers*, Ph.D. Dissertation, Dept. of Chemical Engineering, Yale University, New Haven, CT, 1982.

[16] Gökoğlu, S. A. and Rosner, D. E., "Engineering Correlations of Variable-Property Effects on Laminar Forced Convection Mass Transfer for Dilute Vapor Species and Small Particles in Air," NASA CR-168322, 1984.

[17] Goren, S. L., "Thermophoresis of Aerosol Particles in the Laminar Boundary Layer on a Flat Plate," *Journal of Colloid and Interface Science*, Vol. 61, No. 1, 1977, pp. 77-85.

[18] Rosner, D. E. and Fernandez de la Mora, J., "Small Particle Transport Across Turbulent Nonisothermal Boundary Layers," *Transactions of ASME Journal of Engineering for Power*, Vol. 104, 1982, pp. 885-894.

[19] Fernandez de la Mora, J., *Deterministic and Diffusive Mass Transfer Mechanisms in the Capture of Vapors and Particles*, Ph.D. Dissertation, Dept. of Chemical Engineering, Yale University, New Haven, CT, 1980.

[20] Talbot, L., Cheng, R. K., Scheffer, R. W., and Willis, D. R., "Thermophoresis of Particles in a Heated Boundary Layer," *Journal of Fluid Mechanics*, Vol. 101, 1980, pp. 737-758.

[21] Cole, J. D., *Perturbation Methods in Applied Mathematics*, Springer Verlag, NY, 1968.

[22] Walker, K. L., Homsy, G. M., and Geyling, F. T., "Thermophoretic Deposition of Small Particles in Laminar Tube Flow," *Journal of Colloid and Interface Science*, Vol. 69, No. 1, 1979, pp. 138-147.

[23] Mills, A. F., Hang, X., and Ayazi, F., "The Effect of Wall Suction and Thermophoresis on Aerosol Particle Deposition from a Laminar Boundary Layer on a Flat Plate," *International Journal of Heat and Mass Transfer*, Vol. 27, No. 7, 1984, pp. 1110-1113; see also Gökoğlu, S. A., Rosner, D. E., and Castillo, J., "Discussion," *International Journal of Heat and Mass Transfer* (submitted, 1985).

[24] Belmann, R. E., *Quasilinearization and Nonlinear Boundary Value Problems*, Elsevier, New York, 1965.

[25] Gökoğlu, S. A. and Rosner, D. E., "Viscous Dissipation Effects on Thermophoretically-Augmented Aerosol Particle Transport Across Laminar Boundary Layers," *International Journal of Heat Fluid Flow*, Vol. 6, No. 4, 1985.

[26] Brown, W. B. and Donoughe, P. L., *Tables of Exact Laminar Boundary Layer Solutions When the Wall Is Porous and Fluid Properties Are Variable*, NACA TN 2479, 1951.

[27] Livingood, J. B. and Donoughe, P. L., *Summary of Laminar Boundary Layer Solutions for Wedge-Type Flow Over Convection and Transpiration-Cooled Surfaces*, NACA TN 3588, 1955.

[28] Hartnett, J. P. and Irvine, T. F., Jr., in *Advances in Heat Transfer*, Vol. 4, Academic Press, New York, 1967.

[29] Spalding, D. B., "Mass Transfer Through Laminar Boundary Layers—1. The Velocity Boundary Layer," *International Journal of Heat and Mass Transfer*, Vol. 2, Nos. 1/2, 1961, pp. 15-32.

[30] Spalding, D. B. and Evans, H. L., "Mass Transfer Through Laminar Boundary Layers—2. Auxilliary Functions for the Velocity Boundary Layer," *International Journal of Heat and Mass Transfer*, Vol. 2, No. 3, 1961, p. 199.

[31] Evans, H. L., "Mass Transfer Through Laminar Boundary Layers—3a. Similar Solutions to the b-Equation When $B=0$ and $\sigma>0.5$," *International Journal of Heat and Mass Transfer*, Vol. 3, No. 1, 1961, pp. 26-41.

[32] Evans, H. L., "Mass Transfer Through Laminar Boundary Layers—7. Further Similar Solutions to the b-Equation for the Case $B=0$," *International Journal of Heat and Mass Transfer*, Vol. 5, 1962, p. 35.

[33] Srivastava, R. and Rosner, D. E., "A New Approach to the Correlation of Boundary Layer Transfer Rates with Thermal Diffusion and/or Variable Properties," *International Journal of Heat and Mass Transfer*, Vol. 22, 1979, pp. 1281-1294.

[34] Fernandez de la Mora, J. and Rosner, D. E., "Effects of Inertia on the Diffusional Deposition of Small Particles to Spheres and Cylinders at Low Reynolds Numbers," *Journal of Fluid Mechanics*, Vol. 125, 1982, pp. 379-395.

[35] Rosner, D. E. and Fernandez de la Mora, J., "Inertial Deposition of Particles Revisited and Extended: Eulerian Approach to a Traditionally Lagrangian Problem," *PhysicoChemical Hydrodynamics Journal*, Vol. 2, No. 1, 1981, pp. 1-21.

[36] Rosner, D. E. and Fernandez de la Mora, J., "Correlation and Prediction of Thermophoretic and Inertial Effects on Particle Deposition from Nonisothermal Turbulent Boundary Layers," *Particulate Laden Flows in Turbomachinery*, edited by W. Tabakoff et al., ASME, New York, 1982, pp. 85-94.

[37] Israel, R. and Rosner, D. E., "Use of a Generalized Stokes Number to Determine the Aerodynamic Capture Efficiency of Non-Stokesian Particles from a Compressible Gas Flow," *Journal of Aerosol Science and Technology*, Vol. 2, 1983, pp. 45-51.

[38] Rosner, D. E. and Atkins, R. M., "Experimental Studies of Salt/Ash Deposition Rates from Combustion Products Using Optical Techniques," *Fouling and Slagging Resulting from Impurities in Combustion Gases*, edited by R. Bryers, Engineering Foundation, New York, 1983, pp. 469-492.

[39] Gökoğlu, S.A. and and Rosner, D. E., "Prediction and Rational Correlation of Thermophoretically Reduced Particle Mass Transfer to Hot Surfaces Across Laminar or Turbulent Forced-Convection Gas Boundary Layers," *Chem. Eng. Commun.*, in press 1986.

[40] Gökoğlu, S. A. and Rosner, D. E., "Comparisons of Rational Engineering Correlations of Thermophoretically-Augmented Particle Mass Transfer with STAN5-Predictions for Developing Boundary Layers," ASME 84-GT-158, 29th International Gas Turbine Conference, ASME, Amsterdam, The Netherlands, 1984.

[41] Gökoğlu, S. A. and Rosner, D. E., "Correlation of Thermophoretically-Modified Small Particle Deposition Rates in Forced Convection Systems with Variable Properties, Transpiration Cooling and/or Viscous Dissipation," *International Journal of Heat and Mass Transfer*, Vol. 27, 1984, pp. 639-645.

[42] Rosner, D. E., Gökoğlu, S. A., and Israel, R., "Rational Engineering Correlations of Diffusional and Inertial Particle Deposition Behavior in Nonisothermal Forced Convection Environments," *Fouling of Heat Exchanger Surfaces*, edited by R. Bryers, Engineering Foundation, New York, 1983, pp. 235-256.

[43] Svehla, R. A., "Estimated Viscosities and Thermal Conductivities of Gases at High Temperatures," NASA TR-132, 1962.

[44] Bird, R. S., Stewart, W., and Lightfoot, E. N., *Transport Phenomena*, John Wiley & Sons, New York, 1863; see also D. E. Rosner, *Transport Processes in Chemically Reacting Flow Systems*, Butterworths, Boston, London, April 1986, Volume in Series on Chemical Engineering, edited by H. Brenner.

[45] Hirschfelder, J. P., Curtiss, C. F., and Bird, R. B., *Molecular Theory of Gases and Liquids*, John Wiley & Sons, New York, 1954.

[46] Israel, R. S, *Thermal Diffusion Effects on Fuel Vapor Mass Transport Across Non-isothermal Boundary Layers in Surface-Catalyzed Combustion*, Ph.D. Dissertation, Dept. of Chemical Engineering, Yale University, New Haven, CT, 1983.